

**MT-MRANBRAINTUMORNET: A NOVEL BRAIN TUMOUR AND SEVERITY LEVEL  
CLASSIFICATION FRAMEWORK USING META-HEURISTIC-ASSISTED  
TRANSFORMER BASED MULTISCALE RESIDUAL ATTENTION NETWORK**

**<sup>1</sup>R.Aishwarya, <sup>2</sup>Dr.Sumathi Ganesan , <sup>3</sup> Dr.TKS Rathish Babu**

<sup>1</sup>Research scholar, Faculty of engineering and technology, Department of Computer Science and Engineering,

Annamalai University, Annamalai Nagar, Tamil Nadu, India

<sup>2</sup>.Assistant Professor, Faculty of engineering and technology, Department of Computer Science and Engineering,

Annamalai University, Annamalai Nagar, Tamil Nadu, India

<sup>3</sup>Department of Computer Science and Engineering, Sridevi Womens Engineering college, Hyderabad, India

<sup>1</sup>aishwaryar.rajendran@gmail.com <sup>2</sup>sumi.ganesan@yahoo.com <sup>3</sup>tksbabu80@gmail.com

**Abstract-**Brain tumor is generally structured by the subtle summation of anomalous cells because it categorized as a mass of tissue, and it is very crucial to categorize brain tumors from Magnetic Resonance Imaging (MRI) for diagnosis purpose. The investigation of brain tumors by humans is a routine process for detecting and classifying MRI brain tumors. Due to the low contrast of the images, poor boundaries and noises, the image classification techniques provide poor performance in medical images. Hence, a new classification model for detecting brain tumors is needed to solve the critical challenges in existing approaches. This decreases human intervention while making decisions about brain tumors. Therefore, a new brain tumor classification model is investigated to solve the challenges in existing approaches with deep learning. The proposed framework consists of two main different phases (i) classifying normal and abnormal images and (b) Segmentation and severity classification of abnormal images. The first step is comprised of pre-processing and classification. Firstly, the required images are gathered from the benchmark databases. These collected images are undergone pre-processing, which is done by filtering methods and Contrast Limited Adaptive Histogram Equalization (CLAHE). Subsequently, the pre-processed image is fed into the new classification model as a Transformer-based Multi-scale Residual Attention Network (TMRAN), where the normal and abnormal images are obtained. While in the second case, the classified abnormal image is considered as the input for the segmentation process. The segmented image is obtained by Convolutional Neural Network (CNN), Modified UNet and UNet, in turn the parameters in UNet is optimized by using the Modified Controlling Parameters-based African Vultures Optimization Algorithm (MCP-AVOA), termed as Modified UNet. At the final stage, these segmented images are applied as input to the novel TMRAN model, where the hyper parameters are tuned optimally using improved MCP-AVOA in order to acquire the optimal severity classified results. The performance is validated using diverse measures and compared over

other conventional methodologies. Thus, the findings elucidate that the proposed model attains higher classification results.

Keywords-Brain Tumor Classification; MRI Images; Severity Level Computation; Transformer-based Multi-scale Residual Attention Network; Modified Controlling Parameters-based African Vultures Optimization Algorithm

## **I. INTRODUCTION**

Generally, a brain tumor is a disorder and it is caused by abnormal tissue or cell development in the brain [9]. In the human body, the cells reproduce and die at regular times, where the previous cells are replaced by newer ones. But, fewer cells are continued to grow and become abnormal, which causes brain function damage and it leads to death [10]. There are minimum types of brain tumors available that are 120 types of brain tumors and the disorders to exist in the Central Nervous System (CNS) are epilepsy, brain tumor, sclerosis and so on [11]. Therefore, automatic classification systems are designed to detect brain tumors from the human body to get accurate and fast results [12]. For analyzing brain disorders, MRI is extremely applicable, and is accepted for forwarding and giving anatomical information [13]. To provide high spatial resolution is a challenging task and segmentation of MRI images is also a challenging task.

In addition, image segmentation is highly applicable in various image processing and computer vision applications [14]. During segmentation, the entire image is partitioned into many regions with the help of several metrics and it is useful for further processing [15]. To detect the abnormalities present in the MRI, the image segmentation plays a significant role and many segmentation algorithms provide poor performance because of noise [16]. The low contrast and low resolution images also degrades the performance of segmentation and hence it is difficult to accurately detect the brain tumors [17]. Early diagnosis of brain tumors saves the life of patients but, the appropriate examination of brain tumors from MRI and the examination of patient's condition are challenging [18]. The traditional MRI-based brain tumor detection approaches are highly depend on the doctor's medical expertise and hence it takes more time to provide detection results and it increases the complexity for diagnosing brain tumor with naked human eyes [19]. While processing with huge amount of data, the detection of abnormality level is challenging and it makes fault classification outcomes among these huge volume data. In addition, it increases the computational cost and execution time [20]. Hence, detecting and classifying brain tumors with higher accuracy is highly important and it is done with the help of Computer-Aided Diagnostic (CAD) systems and these CAD systems save the life of human lives [21].

In the field of computer science, artificial intelligence allows thinking, learning, and rectifying issues from various sources. For detecting and diagnosing brain tumors, artificial intelligence plays a significant role, and it automatically classifies the MRI images [22]. More attempts are made to provide a highly accurate and reliable technique for the detection and classification of brain tumors. The varying features of shape, contrast and texture make it difficult to rectify the issues. Deep and machine learning strategies are the subset of artificial intelligence [23]. These techniques consist of steps like preprocessing of images, retrieval of features, selection of features,

dimensionality reduction and classification. The most widely adopted Deep learning with neural networks provides promising results and it provides efficient outcomes in the detection of brain tumors [24]. The features from MRI are very effectively learned with the help of Convolutional Neural Networks (CNNs) and it is helpful to provide high precision. Deep learning has very well in object detection, pattern categorization, decision-making tasks, and voice recognition and hence it is suitable for the recognition of brain tumors [25]. In the healthcare industry, the machine learning approaches performed well in the detection of brain tumors that includes “Support Vector Machines (SVMs), Naive Bayes and K-Nearest Neighbor (k-NN), decision trees”, and also deep learning with the versions of CNN includes GoogleNet, VGGNets, and ResNets. But, these techniques are suffered from the challenges like low accuracy, high computational costs, as well as slow learning ability. In addition, security and privacy are the greatest issues while storing medical data in the cloud environment. Providing greater precision and accuracy is the critical issue in dealing with the detection and severity level classification of brain tumors. These challenges are rectified with the usage of a newly recommended brain tumor detection and severity classification model using deep learning.

The important contributions of the developed brain tumor classification model using deep learning algorithms are summarized below.

- To design a brain tumor detection and severity classification model to identify the brain tumor from the segmented images and classify the severity of the brain tumor to provide proper treatment based on the severity.
- To develop an MCP-AVOA to optimally selects the parameters during the classification and segmentation stage to enhance the effectiveness of the suggested brain tumor detection and severity classification scheme.
- To design a brain tumor classification stage using TMRAN, where the parameters from TMRAN are tuned with the help of MCP-AVOA for maximizing the classification accuracy on classifying the brain tumor diseases.
- To segment the images using deep networks, where CNN, Modified UNet and Unet are utilized for segmenting the images with higher dice coefficient and jacard index. The parameters from Modified UNet are only optimized via MCP-AVOA to improve the segmentation efficiency.
- To make sure the effectiveness of the investigated MCP-AVOA-TMRAN-based brain tumor detection and severity classification model, the performance analysis is carried out over various algorithms.

The balancing sections used in the proposed MCP-AVOA-TMRAN-based brain tumor classification model are summarized as below. The traditional brain tumor classification approaches via the utilization of deep learning with advantages and disadvantages are provided in Section II. The architectural description and the dataset collection with preprocessing stages are explained in Section III. The deep networks-based brain tumor classification and proposed algorithm explanation are described in section IV. The segmentation steps and severity level

classification process are explained in Section V. The performance analysis is encapsulated in Section VI and the conclusion of the suggested brain tumor detection and severity classification approach is given in Section VII.

## **II. LITERATURE SURVEY**

### **A. Related Works**

In 2022, Shah et al. [1] have introduced a robust approach for the detection of brain tumors from MRI images with the utilization of fine-tuned EfficientNet. With various filter sizes, the image enhancement methodologies were provided over the MRI images. The data samples have been increased by using image augmentation techniques. The final stage detection has been carried out via the deep CNN called as EfficientNet model. Better detection results were obtained by using this EfficientNet than other classifiers.

In 2022, Musallam et al. [2] have offered an automatic brain tumor classification model by using CNN from MRI images. It is highly suitable for the diagnosis of meningioma, glioma, and pituitary. For fast training, the network used the batch normalization layer with ease of initialization and a higher learning rate. The developed network was a lightweight network because it required a small number of training iterations. The robustness and detection accuracy of the offered scheme was high when compared to other models.

In 2022, Ramprasad et al. [3] have recommended a deep probabilistic sensing and learning model for classifying brain tumors with the assistance of Fusion-net and segmentation mechanism. Here, the MRI and the CT images were fused to classify the brain tumors. The segmentation of images has been carried out with the utilization of fuzzy c-means and K-means clustering. From the segmented regions, the hybrid features have been extracted and given to a deep probabilistic neural network to classify and diagnose brain tumors. The segmentation and classification accuracy of the developed model was high.

In 2019, Mallick et al. [4] have suggested a brain MRI classification approach for detecting cancers with the usage of an autoencoder-based deep neural network. Here, the deep wavelet encoder has been utilized for achieving image compression property and image decomposition properties. The classification process has been done with the utilization of DNN. The results were shown that the proposed model outshined the other models.

In 2020, Chaudhary and Bhattacharjee [5] have introduced a brain tumor detection approach by using K-means clustering and Discrete Wavelet Transform (DWT). Initially, image segmentation has been executed using clustering. Then, brain tumor identification was carried out using SVM. It has provided greater accuracy than other models.

In 2022, Manoj and Dhas [6] recommended an automatic brain tumor segmentation approach for detecting malignancy via 3D MRI with the utilization of adaptive 3D-UNet with DNN. Here, the hybridized optimization algorithm has been adopted to improve the efficacy of the detection and classification of brain tumors. The developed model satisfied several multi-objective functions during the segmentation and the most appropriate features have been extracted using the developed

model. After the final stage, classification was performed and the results have proven its effectiveness.

In 2021, Deepak and Ameer [7] have introduced an automatic brain tumor categorization method from MRI images using CNN and SVM. In this, the CNN network has been assisted in the extraction of features from the MRI images. For enhancing the performance of the system, the SVM classifier has been utilized to detect brain tumors. At last, the overall classification accuracy of the developed model was high when analyzed with the traditional models.

In 2020, Amin et al. [8] have offered a brain tumor detection model with the help of Long Short Term Memory (LSTM) using MRI images. Initially, the Gaussian filters were used to increase the quality of MRI images. The LSTM with four layers was used for the identification and classification of brain tumors. The performance of the detection of brain tumors has been improved by optimizing the hidden neurons. The results confirmed that the developed model had provided a higher classified score than existing approaches.

### **B. Problem statement**

The abnormal brain cell growth causes brain tumors. Moreover, the survival rate of patients is mainly affected with the brain tumor. The manual identification of brain tumors is more tedious as well as time-consuming and it is challenging to detect the brain tumor from complex data. The traditional approaches are highly prone to errors. Therefore, several computer vision-based brain tumor detection approaches have been developed to solve the challenges in manual classification approaches. The features and challenges of existing brain tumor detection models are summarized in Table I. EfficientNet [1] effectively detects infrequent brain tumor cells with higher accuracy. Furthermore, it reduces the overfitting problem by using a data augmentation technique. But, it requires the segmentation of images to reduce time complexity. For instance, it is not suitable to process with other imaging techniques like CT, ultrasound and X-ray. DCNN [2] is highly applicable for the diagnosis of pituitary, meningioma and glioma. In addition, it timely detects brain abnormalities with higher detection accuracy. Yet, it does not provide sufficient accuracy while processing large dimensional datasets. On the other hand, it is not possible to detect the brain tumor from CT, ultrasound and X-ray. A deep probabilistic neural network [3] effectively detects the tumor region from the fused images. Nevertheless, it is highly applicable for real world applications. However, it needs detailed feature extraction techniques to improve the detection accuracy. DNN [4] provides high sensitivity, accuracy, specificity and precision. Moreover, it effectively satisfies the image decompression property. Hence, it takes more time to provide detection results. Furthermore, the computational overhead of the system is high. SVM [5] provides highly robust results in the categorization of brain MRI images. In addition, the noise present in the system is effectively handled with the help of a developed model. Nonetheless, the distinct boundaries are not effectively handled with the help of using an SVM classifier. In addition, there is a chance for misclassification errors. DNN [6] improves the segmentation performance in terms of MSE, PSNR, SSIM and dice coefficient. Consequently, it enhances the image contrast, and hence the detection performance is highly enhanced. But it requires more

training time. SVM [7] has lesser computation and memory requirements. Moreover, the classification accuracy over the detection of brain tumors is high. On the other hand, the distinct boundaries are not effectively handled with the help of using an SVM classifier. Subsequently, there is a chance for misclassification errors. LSTM [8] is mainly useful in stroke and glioma detection. For instance, it gives better outcomes while learning temporal data processing. Yet, it does not measure the severity level of the diseases. Consequently, subtumoral region classification is not possible in the developed model. These challenges are rectified by the newly developed brain tumor classification system using deep learning from MRI images.

**TABLE I. MERITS AND DISADVANTAGES OF TRADITIONAL BRAIN TUMOR DETECTION APPROACHES USING DEEP LEARNING**

Author [citation]	Methodology	Features	Challenges
Shah <i>et al.</i> [1]	EfficientNet	<ul style="list-style-type: none"> <li>It effectively detects infrequent brain tumor cells with higher accuracy.</li> <li>It reduces the overfitting problem by using a data augmentation technique.</li> </ul>	<ul style="list-style-type: none"> <li>It requires the segmentation of images to reduce time complexity.</li> <li>It is not suitable to process with other imaging techniques like CT, ultrasound and X-ray.</li> </ul>
Musallam <i>et al.</i> [2]	DCNN	<ul style="list-style-type: none"> <li>It is highly applicable for the diagnosis of pituitary, meningioma and glioma.</li> <li>It timely detects brain abnormalities with higher detection accuracy.</li> </ul>	<ul style="list-style-type: none"> <li>It does not provide sufficient accuracy while processing with large dimensional datasets.</li> <li>It is not possible to detect the brain tumor from CT, ultrasound and X-ray.</li> </ul>
Ramprasad <i>et al.</i> [3]	Deep probabilistic Neural network	<ul style="list-style-type: none"> <li>It effectively detects the tumor region from the fused images.</li> <li>It is highly applicable to real word applications.</li> </ul>	<ul style="list-style-type: none"> <li>It needs detailed feature extraction techniques to improve detection accuracy.</li> </ul>
Mallick <i>et al.</i> [4]	DNN	<ul style="list-style-type: none"> <li>It provides high sensitivity, accuracy, specificity and precision.</li> <li>It effectively satisfies the image decompression property.</li> </ul>	<ul style="list-style-type: none"> <li>It takes more time to provide detection results.</li> <li>The computational overhead of the system is high.</li> </ul>
Chaudhary and Bhattacharjee [5]	SVM	<ul style="list-style-type: none"> <li>It provides highly robust results over the categorization of brain MRI images.</li> <li>The noise present in the system is effectively handled by using the suggested approach.</li> </ul>	<ul style="list-style-type: none"> <li>The distinct boundaries are not effectively handled with the help of using the SVM classifier.</li> <li>There is a chance for misclassification errors.</li> </ul>
Manoj and Dhas [6]	DNN	<ul style="list-style-type: none"> <li>It improves the segmentation performance in terms of MSE, PSNR, SSIM and dice coefficient.</li> <li>It enhances the image contrast, and hence the detection performance is highly enhanced.</li> </ul>	<ul style="list-style-type: none"> <li>It requires more training time.</li> </ul>
Deepak and Ameer [7]	SVM	<ul style="list-style-type: none"> <li>It has lesser computation and memory requirements.</li> </ul>	<ul style="list-style-type: none"> <li>It extends the training time.</li> </ul>

		<ul style="list-style-type: none"> <li>The classification accuracy over the detection and classification of brain tumors is high.</li> </ul>	<ul style="list-style-type: none"> <li>It needs data augmentation to provide significant results.</li> </ul>
Amin <i>et al.</i> [8]	LSTM	<ul style="list-style-type: none"> <li>It is mainly useful in stroke and glioma identification.</li> <li>It gives superior outcomes while learning temporal data processing.</li> </ul>	<ul style="list-style-type: none"> <li>It does not compute the severity level of the diseases.</li> <li>Subtumoral region classification is not possible in the developed model.</li> </ul>

### III. A NOVEL BRAIN TUMOUR DETECTION AND SEVERITY LEVEL CLASSIFICATION USING META-HEURISTIC ASSISTED DEEP LEARNING

#### A. Brain Tumour Detection and Severity Classification Model

The main step in analyzing MRI is medical imaging. It is very helpful for the diagnosis of brain tumors. Initially, the MRI images contain statistical features and hence to deal with the analysis of these statistical features is slightly different. The structure of the brain is very complex and it is difficult to analyze the complex patterns from the MRI images. Moreover, researchers face a lot of challenges because of the immense processes of huge volumes of data. In addition, the size and shape are recognized with inter-class and intra-class variabilities. These are effectively handled with the help of hybrid approaches. In addition, the traditional brain tumor detection approaches using deep learning struggle with overfitting and generalization issues. Many deep learning techniques are suggested to reduce human intervention and time-consuming. The affected portion from the MRI images is difficult to detect. The better feature extraction techniques have the ability to detect abnormal regions. To provide accurate brain tumor classification results, a new brain tumor detection and severity classification model is implemented with the help of deep learning. The structural view of developed brain tumor detection and severity classification using deep learning is given in Fig. 1.

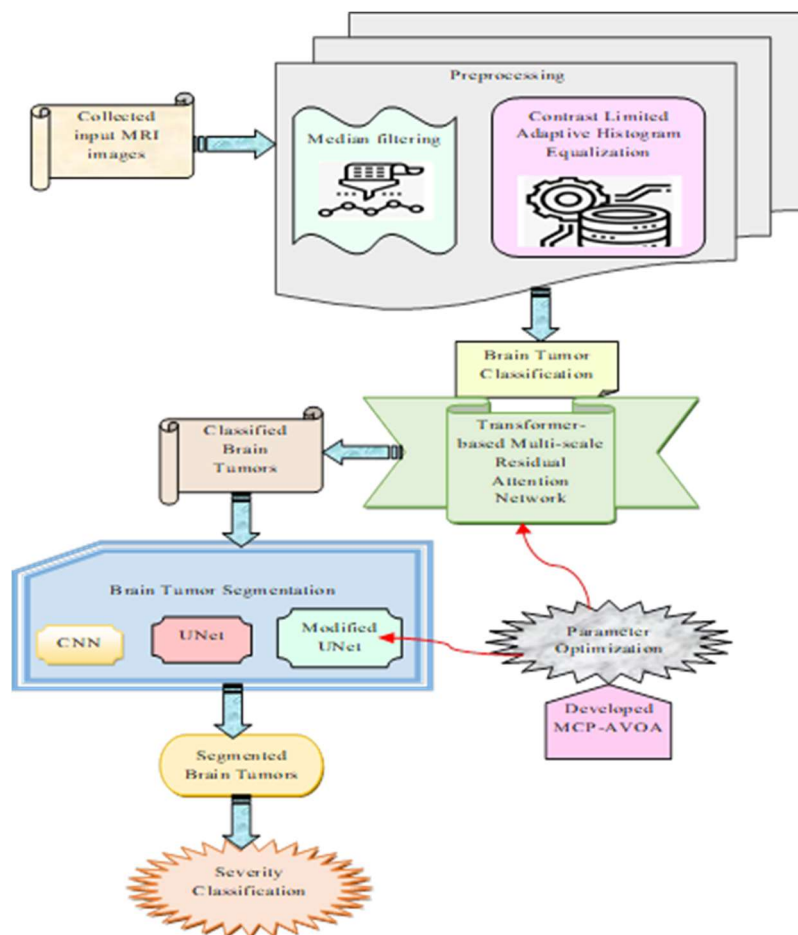


Fig. 1. Architecture of implemented Brain Tumor Classification System using deep learning

A new brain tumor detection and severity classification model is developed to identify the abnormalities and severity level classification from MRI images by the utilization of a deep learning algorithm. The classification accuracy over the detection of abnormal and normal cases is high when compared to the traditional approaches. At first, the MRI images are acquired from various online databases and the quality of MRI images is enhanced with the help of median filtering and CLAHE. The preprocessed images are given to TMRAN to classify the complex MRI images for the identification of brain tumors. The hidden neuron count, batch size and epoch counts from TMRAN are tuned with the help of developed MCP-AVOA to improve the classification accuracy and decrease FNR as well as FPR. The classified images are fed to the abnormal region segmentation process for identifying the severity level of the images, where CNN, Modified UNet and Unet are utilized for segmenting the images. Here, the hidden neuron count, epoch count and steps per epoch from UNet are tuned with the utilization of developed MCP-AVOA. The tuned parameters from UNet improve the dice coefficient and jacard index. Finally, the severity of the diseases is classified in the model to provide a proper diagnosis of brain tumors. The effectiveness of the implemented model is compared with the traditional brain tumor detection algorithms and



classifiers to validate the effectiveness of the developed brain tumor detection and severity classification scheme.

**B. Brain Tumour Dataset Description**

There are three different datasets considered for the detection of brain tumors.

Dataset (Brain Tumor Classification MRI): It is obtained from the online source of “Brain Tumor Classification (MRI) | Kaggle,”: accessed on 2023-05-29. Brain tumor is considered as the most aggressive disorder and it affects adults as well as children. It contains the MRI data and the images of the brain tumor are partitioned into testing and training folders. Four subfolders are included in each folder. It contains images of respective tumor classes. The testing folder consists of four directories such as glioma, meningioma, not tumor and pituitary tumor. The training folder also consists of four directories and the version of this dataset is Version 2 (93.08 MB).

The collected data are indicated by the term  $MR_c^{CL}$ ,  $c = 1,2,3...C$  be the total amount of acquired images. The collected sample MRI images are given in Fig. 2.

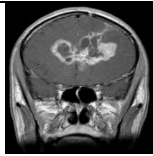
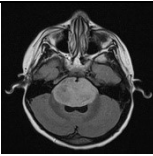
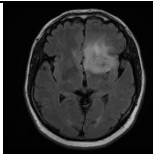
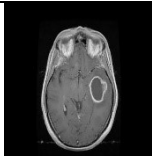
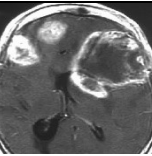
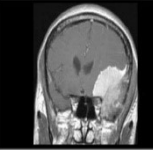
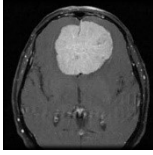
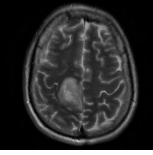
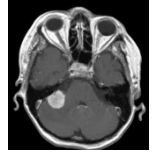
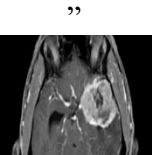
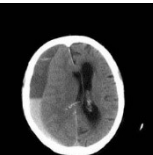
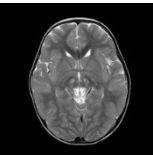
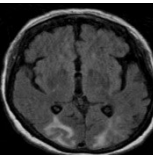
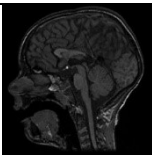
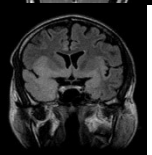
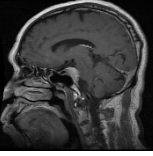
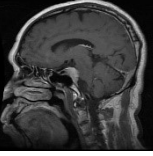
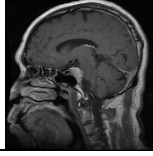
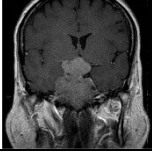
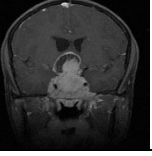
Gathered MRI images	1	2	3	4	5
Glioma Tumor					
Meningioma tumor					
No tumor					
Pituitary Tumor					

Fig. 2. Sample images attained from three datasets

**C. Preprocessing over Raw Images**

Image preprocessing is helpful for improving the quality of images by surpassing the unwilling distortions from the collected images. This enhanced quality of images is helpful for further classification of MRI images to detect brain tumors very accurately. Here, two image

preprocessing approaches are adopted to improve the quality of images that are Median filtering and CLAHE.

Median filtering: The MRI images to be given to the median filtering approach are . Most commonly, a median filter is a nonlinear filter where all the input values are evaluated through the median value of input samples based on the window size. Then, the middle values are sorted. It effectively decreases the random noise and also the periodic patterns are decreased with the help of the median filter. It is mainly helpful for decreasing the amount of intensity variation from one pixel to another pixel with the estimated median value. The median filtered MRI image is indicated by .

CLAHE: It is one of the image preprocessing methods for improving the contrast of the MRI images. The input to be given to the CLAHE is median filtered images . It calculates the histogram values and it corresponds to the distinct portions of the images. It distributes the luminance values of the images. It functioned very well on the small portion of the images that are called tiles. The false boundaries in the images are removed by using the bilinear interpolation, where the surrounding tiles are blended by using this algorithm. There are two parameters effectively used in this CLAHE that are block size and clip limit. The quality of the image is improved by using these parameters. The quality improved image after performing CLAHE is indicated by the term .

#### **IV. NORMAL AND ABNORMAL LEVEL CLASSIFICATION USING TRANSFORMER-BASED MULTI-SCALE RESIDUAL ATTENTION NETWORK**

##### **A. Transformer-based Multi-scale Residual Attention Network**

The multi-scale RAN is used in the offered model to classify the MRI images for finding the affected region of brain tumors. The multi-scale RAN [32] consists of two branches the trunk and the attention branch. In the trunk branch, the process of feature extractions is carried out by employing multi-scale convolutions. The attention branch is comprised of the integration of both channel and position attention. The number of channels in the input feature maps is adjusted through multi-scale convolutions with layers. By using channel split, the created feature maps are identically partitioned into M number of groups. The features are extracted through these grouped feature maps.

In this, the global information is attained through the position-based attention structure. The feature map in all the channels represents the special feature detector and the network channel attention gets more attention to extract the useful information from the features. The outcome of the channel attention map is indicated by . In the position attention mechanism, the applied input feature maps are passed to the mean and maximum layers for acquiring feature maps. The position attention modules not only raise the networks' receptive field. Moreover, it introduces a huge number of parameters and also the nonlinearity of the network is increased. Finally, new position weights are obtained using the concatenation layer. The interference information is suppressed in the developed approach and it is denoted as . With the help of channel attention, the weight values are effectively suppressed. The implementation process with the help of two constitutes is given in Eq. (1).

$$AT(z) = C(z) \times N(z) \quad (1)$$

This can be described that not only serves as a feature selector and it updates the gradient filter during forward interference and backpropagation. The element-wise multiplication is carried out between the channel and position attention module to attain the weighted attention map. The fine-tuning of features is carried out in the residual block and it is implemented in Eq. (2).

$$FT(z) = (1 + AT(z)) \times S(z) \quad (2)$$

Here, the term indicates the output of the trunk branch. The meaningful information from the MRI is extracted using the trunk and attention branches. The transformer is an encoder and decoder network and it consists of two sublayers in its encoder. In the first sublayer, the multi-head attention module is presented, and it computes the output embeddings based on the key values. The multi-head attention is given in Eq. (3).

$$MHd(U, V, Z) = \text{Concat}(hd_1, \dots, hd_f) R^o \quad (3)$$

Here, the term is described in Eq. (4).

$$hd_1 = \text{Atm}(UR_a^u, VR_a^v, ZR_a^u) \quad (4)$$

Here, and are the matrices with a dimension of and is a matrix with the dimension of , respectively. The linear transformation of matrices is carried out with the help of a matrix.

The attention function is implemented on the basis of a scaled dot-product with attention module and it computes the weighted sum values that are represented in Eq. (5).

$$\text{Atm}(U^*, V^*, Z^*) = \text{Soft max} \left( \frac{U^* V^{*o}}{\sqrt{p_t}} \right) Z^* \quad (5)$$

Here, the raw attention scores are presented in the query and key pair, which is denoted by the term . These scores are normalized with the help of the softmax function. The feed-forward with hidden layers in the fully connected network is presented in the fully connected feed-forward layer. The schematic illustration of a multi-scale transformer-based residual attention network is showcased in Fig. 3.

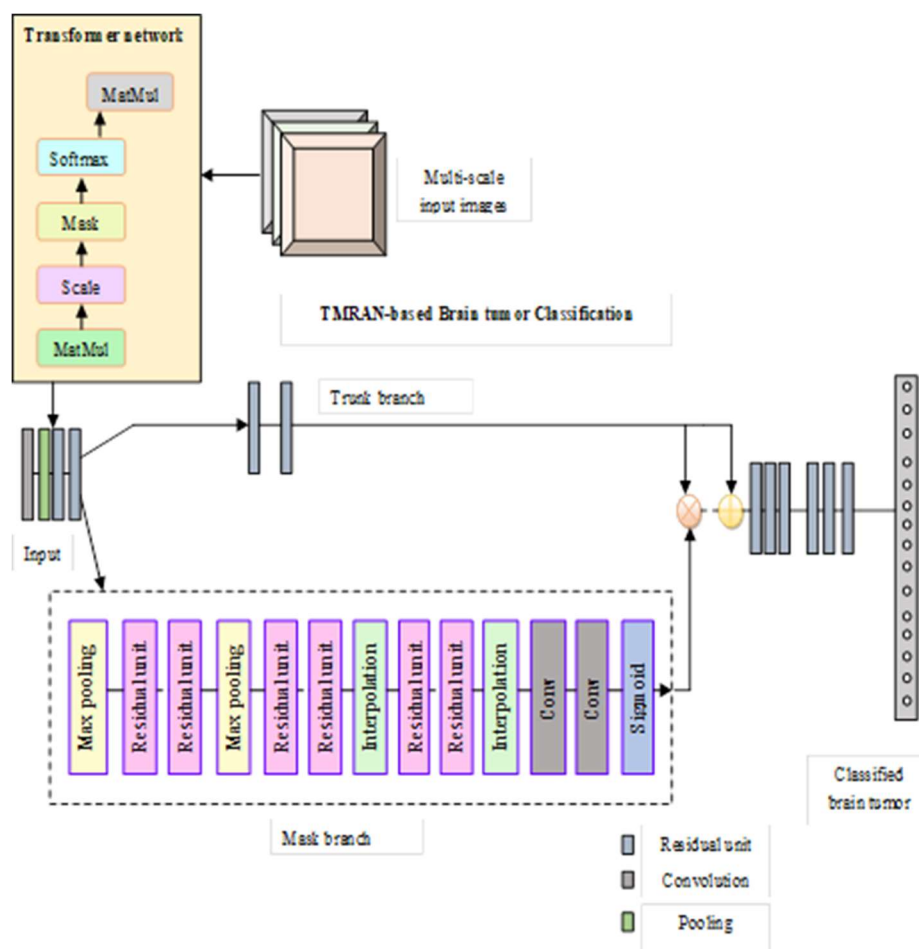


Fig. 3. Block schematic representation of Transformer-based Multi-scale RAN

### B. Proposed TMRAN for Brain Tumor Classification

To detect the brain tumor, the developed TMRAN model is used. The developed TMRAN effectively classify the MRI and provides outcome as normal and abnormal regions. The network sequences, such as hidden neuron count, number of epochs and batch size in TMRAN, are optimally tuned with the help of designed MCP-AVOA for improving the classification performance. Here, the evaluation is estimated in between the target labels and classification score to estimate the objective function. The main objective of using TMRAN-based classification with hyperparameters tuning is improving the accuracy and minimizing FNR, FDR and FPR. The objective function of using parameter optimized brain tumor classification process is expressed in Eq. (6).

$$F_1 = \underset{(H_{uv}^{RAN}, E_{uv}^{RAN}, B_{uv}^{RAN})}{\operatorname{arg\,min}} \left( \frac{1}{Ar} + FNR + FPR + FDR \right) \quad (6)$$

Here, the optimized hidden neurons from TMRAN are denoted by ranges between , the tuned count of epochs from TMRAN is represented by that lies in and the tuned batch size from TMRAN is

signified as in between . In addition, the term signifies classification accuracy and it is evaluated through Eq. (7).

$$Ar = \frac{(A_{po} + A_{ng})}{A_{po} + A_{ng} + B_{po} + B_{ng}} \quad (7)$$

$$FNR = \frac{B_{po}}{B_{po} + A_{po}} \quad (8)$$

$$FPR = \frac{B_{po}}{B_{po} + A_{ng}} \quad (9)$$

$$FDR = \frac{A_{ng}}{A_{ng} + B_{po}} \quad (10)$$

The “true positive observation, true negative observation, false positive observation and false negative observation” is denoted by  $A_{po}$ ,  $A_{ng}$ ,  $B_{po}$  and  $B_{ng}$ , respectively.

### C. Proposed MCP-AVOA

The developed MCP-AVOA is used in the brain tumor detection and severity classification model, to increase the learning ability of complex patterns from the MRI. Therefore, the detection performance is highly enhanced with the help of using this parameter optimization. During classification of brain tumors, the parameters including hidden neuron count, count of epochs and batch sizes from TMRAN are tuned via MCP-AVOA to improve the classification accuracy and minimize FPR, FNR and FDR. During segmentation, the hidden neuron count, count of epochs and steps per epochs from modified UNet are tuned using MCP-AVOA to improve the dice coefficient as well as the jacard coefficient. The AVOA algorithm is suggested for the optimization of parameters because it provides higher balancing in exploration and exploitation phases. But in order to improve the convergence rate and better optimization ability, the controlling parameters used in AVOA are updated in the developed MCP-AVOA. The updating of controlling parameters is done with the support of worst and best fitness functions. The updated formulas for the controlling parameters are described in Eq. (11), Eq. (12), and Eq. (13) correspondingly.

$$Pb_1 = \frac{BstFit}{(WrstFit \wedge 3)} \quad (11)$$

$$Pb_2 = \frac{BstFit}{(WrstFit + 3)} \quad (12)$$

$$Pb_3 = \frac{WrstFit}{(Pb \wedge 3)} \quad (13)$$

The best fitness function is indicated by and the worst fitness is signified as . The optimization and learning ability of these fitness-based controlling parameters is high. Moreover, the convergence rate of this algorithm is also high when compared to traditional AVOA.

AVOA: It is a Metaheuristic algorithm and it is described via robust theories and concepts. The number of vultures is considered as . The count of vultures is partitioned into groups, where the algorithm first evaluates the solutions’ fitness function. After calculating the fitness function, the initial population is divided into various classes. The best vultures are determined by that. The

tendency of the African vultures is defined by the escaping characteristics of vultures. The basic four assumptions formulating AVOA are summarized as follows.

Initially, estimate the best vulture in any group. This can be accomplished by forming the initial population. Here, the entire population of vultures is recalculated in fitness iterations and it is given in Eq. (14).

$$T(q) = \begin{cases} BstVult_1 & \text{if } m_q = H_1 \\ BstVult_2 & \text{if } m_q = H_2 \end{cases} \quad (14)$$

The probability of preferring the chosen vultures to migrate towards other vultures is denoted in the above Eq. (15).

$$m_q = \frac{G_q}{\sum_{q=1}^v G_q} \quad (15)$$

It represents the increased intensification in AVOA.

In the second phase, the starvation rate of vultures is described. Initially, the vultures have high energy and then they go for long distance to search for their food. If the vultures are hungry, then it does not fly long because they did not have sufficient energy. This behavior is mathematically modeled in Eq. (16).

$$n = l \times \left( \sin^{\sigma} \left( \frac{\pi}{2} \times \frac{Itrn}{MaxItrn} \right) + \cos \left( \frac{\pi}{2} \times \frac{Itrn}{MaxItrn} \right) - 1 \right) \quad (16)$$

The rate of satiation of vultures is given in Eq. (17).

$$S = (2 \times Rn_1 + 1) \times Z \times \left( \left( 1 - \frac{Itrn}{MaxItrn} \right) \right) + n \quad (17)$$

The satiation state of vultures is denoted by  $S$ ,  $n$  is the current iteration count and  $l$  is the total iteration count and  $\sigma$  is the random attribute in between  $[-1, 1]$ .

In the third phase, the exploration ability of AVOA is described, where the vultures have high visual ability to find their food. Here, vultures use two strategies based on the parameter  $Pb_1$ . If  $Pb_1$  is greater than or equal to  $Rn_{pb_1}$ , then it follows the condition in Eq. (18).

$$Pb(q+1) = \begin{cases} T(q) - E(q) \times S & \text{if } Pb_1 \geq Rn_{pb_1} \\ T(q) - S + Rn_2 \times \left( (U_b - L_b) \times Rn_3 \right) + L_b & \text{if } Pb_1 < Rn_{pb_1} \end{cases} \quad (18)$$

The best vulture is denoted by  $T(q)$ ,  $E(q)$  is the position of vultures in the next iteration and  $S$  is estimated from Eq. (19).

$$E(q) = |W \times T(q) - Pb(q)| \quad (19)$$

The term  $W$  is the coefficient vector that raises the motion in random and it is the place the vultures migrate randomly to protect food from others. The upper and lower bound are indicated by the variables  $U_b$  and  $L_b$  and correspondingly.

In the exploitation stage, the efficiency of vultures is investigated. This stage has two phases, where the parameter  $Rn_1$  describes the first phase and the parameter  $Rn_2$  describes the second phase. The two phases are rotating flight and siege flight. The first strategy is given in Eq. (20).

$$Pb(q+1) = \begin{cases} E(q) \times (S + Rn_4) - u(q) & \text{if } Pb_2 \geq Rn_{pb_1} \\ T(q) - (R_1 + R_2) & \text{if } Pb_3 < Rn_{pb_1} \end{cases} \quad (20)$$

The satiation rate of vultures is denoted by the randomly distributed number in the interval of . The term is determined using Eq. (21).

$$u(q) = T(q) - Pb(q) \quad (21)$$

The rotational flight mode is described by the spiral model has been used. The terms and is estimated using the below Eq. (22) and Eq. (23), respectively.

$$R_1 = T(q) \times \left( \frac{Rn_5 \times Pb(q)}{2\pi} \right) \times \cos(Pb(q)) \quad (22)$$

$$R_2 = T(q) \times \left( \frac{Rn_6 \times Pb(q)}{2\pi} \right) \times \sin(Pb(q)) \quad (23)$$

The term is estimated using Eq. (24).

$$Pb(q+1) = T(q) - (R_1 + R_2) \quad (24)$$

In the exploitation phase, the vulture movements are described. The exploitation phase is given in Eq. (25).

$$Pb(q+1) = \begin{cases} \frac{B_1 + B_2}{2} & \text{if } Pb_3 \geq Rn_{pb_1} \\ T(q) - |E(q)| \times S \times LV(E) & \text{if } Pb_3 < Rn_{pb_1} \end{cases} \quad (25)$$

The levy flight is indicated by , and the distance of the vulture is signified by the term . The terms and are evaluated through Eq. (26) and Eq. (27), respectively.

$$B_1 = BstVL_1(q) - \frac{BstVL_1(q) \times P(q)}{BstVL_1(q) - P(q)^2} \times S \quad (26)$$

$$B_2 = BstVL_2(q) - \frac{BstVL_2(q) \times P(q)}{BstVL_2(q) - P(q)^2} \times S \quad (27)$$

The position of best vultures is denoted by the term . Here, the controlled parameters and are updated using the newly developed concept. The pseudocode of the offered MCP-AVOA is given in Algorithm 1. The flowchart of implemented MCP-AVOA is demonstrated in Fig. 4.

<b>Algorithm 1: Offered MCP-AVOA</b>	
Load the maximum number of iterations $ITR_{MAX}$ and population size $Pn_{sz}$	
Initialize the location of vultures	
Load the initial population of vultures in the search space	
Evaluate the fitness observation of vultures	
While ( $r < condition\ not\ met$ )	
	For $c = 1$ to $ITR_{MAX}$
	For $d = 1$ to $Pn_{sz}$
	Find the first best position of vultures
	Find the second best position of vultures
	For all vultures
	Select $T(q)$ value in search space using Eq. (14)
	Update the function $S$ using Eq. (17)
	<b>Update the controlling parameters based on Eq. (11), Eq. (12) and Eq. (13).</b>

		<b>Update the location of the vultures based on the controlling parameters</b>
	End For	
	End For	
	End For	
	$r = r + 1$	
	End while	
	Return solution	

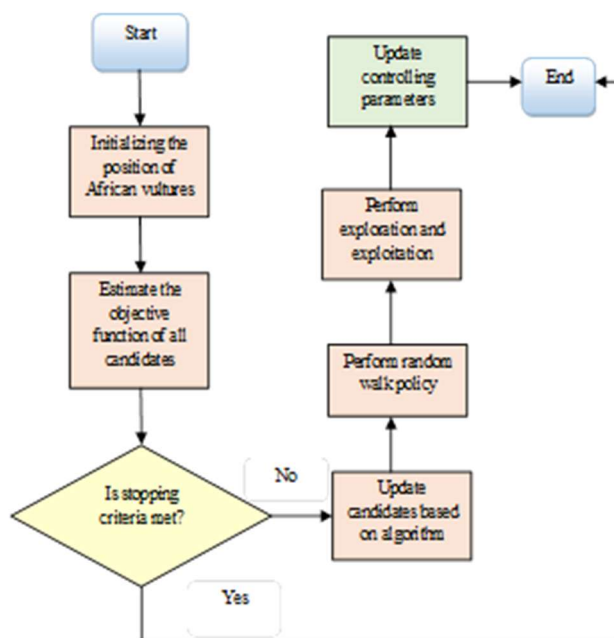


Fig. 4. Flowchart of implemented MCP-AVOA

## V. ABNORMAL REGION SEGMENTATION USING ENSEMBLE CLUSTERING WITH DEEP NETWORKS

### A. Abnormal Region Segmentation

The abnormal regions from the MRI images are definitely identified with the help of TMRAN-based classification and the obtained abnormal regions are given to segmentation. In this developed brain tumor detection model, the abnormal region segmentation is carried out via the utilization of three types of deep networks such as CNN, Modified UNet and UNet. The abnormal region segmentation with the help of these networks is helpful for calculating the severity level of brain tumors.

**CNN [33]:** In CNN, pixel-level segmentation is carried out over the MRI images. The process of labeling each pixel with the appropriate class is stated as the pixel segmentation and pixel fusion is performed with the same tags in the region. The CNN network includes a convolutional layer and fully connected layers. To segment the images with higher accuracy, the encoder and decoder model is introduced in the CNN network. Furthermore, the performance of the segmentation process is improved by using the additional layers in the network. The input image features are extracted using the encoder part and these features are utilized by the decoder network to



reconstruct the segmented images. The skip connections are used to forward the extracted deep features from the encoder network to the decoder network.

In the encoder portion, three convolutional blocks are presented. Two convolutional layers are presented in each block and then the ReLU layer is presented. The ReLU layer is performed as an activation module. The feature resolution of the images is decreased by adding the strided convolution layer at the end of each convolutional block. The main function of using this strided convolution layer is to accelerate the input for the training process. In the decoder part, in addition to that convolutional blocks, task-specific layers are included. Here, the deconvolutional layers are used to increase the feature resolution of the images and are placed before the of convolutional layers. This solution is helpful for reconstructing the segmented MRI images. Retrieved features from the encoder are transferred via the skip connections to the decoder and feature mapping is performed in the decoder part. The features are fused and concatenated with the kernel size . In the softmax layer, the segmented image is generated. This CNN-based segmentation preserves the same resolution of the images. The tiny tumors are effectively identified by using this CNN-based segmentation.

UNet [35]: The U-shaped architecture consists of a specific encoder and decoder. The spatial dimensions in every layer are decreased by the encoder, and it increases the channels. The spatial dims are increased by the decoder by decreasing the channels. The passage of tensors in the decoder is called the bottleneck. The spatial dims are effectively restored to make prediction in every pixel in the input images. The encoder path is known as the contracting path and the decoder path is known as the expansive path. In the encoder, ReLU follows two convolutions and a batch normalization layer. The maximum pooling operation is applied in the network to decrease the spatial dimensions. The feature channel numbers are doubled at each down-sampling step. In the decoder path, it contains upsampling of the feature maps with a convolutional layer. The convolution is used to amp the channel with the appropriate classes in the final layer. In Unet, the entire pixel is grouped with a specific category and it perfectly solves the segmentation tasks. Here, the element wise classification is performed on the multiple features in the decoder. Moreover, securing the learnable parameters in the feature extractors is carried out and it is inferred to provide segmentation outcomes at same resolution. In the given UNet structure, all the neurons are connected to the neurons in the previous layer. Here, all the neurons has the own weight factor. The tiny weight matrix function is utilized for the convolution operation. Based on the convolution core matrix, the convolutional layer summarizes the component-wise product results for all the image fragments. In this UNet, the weight coefficients used in the convolutional kernel are unknown during the training process. The convolution operation is given in below Eq. (28).

$$(U * R)_{ab} = \sum_{h=1}^f \sum_{k=1}^l R_{h,k} \times U_{a+h-1,b+k-1} \quad (28)$$

The two dimensional image is denoted by the term size , and . The filter field is expanded to allow more background information for the calculation. Here, leaky ReLU is also used to calculate the convolutions across the network. Standard batch normalization is used in the network to solve the

memory constraint requirements. The overfitting issues are decreased by using a dropout layer with 12 regularizations.

Modified UNet: The parameters from UNet are optimized with the help of suggested MCP-AVOA and hence it is named Modified UNet. The parameters such as hidden neuron count, epoch count and steps per epoch are optimized from Modified UNet for improving the dice coefficient and jacard index while segmenting the images. The significant goal of optimizing parameters in this UNet is to improve the dice coefficient and jacard index. The objective of this modified UNet-based segmentation process is represented in Eq. (29).

$$F_2 = \underset{\{H_{th}^{MUNet}, E_{th}^{MUNet}, Sp_{k}^{MUNet}\}}{\operatorname{argmin}} \left( \frac{1}{DC + JR} \right) \quad (29)$$

The tuned hidden neuron count from UNet is signified by the term  $H_{th}^{MUNet}$  in between  $E_{th}^{MUNet}$  and  $Sp_{k}^{MUNet}$ , which is the optimized number of epochs in UNet between  $E_{th}^{MUNet}$  and  $Sp_{k}^{MUNet}$  is the optimized steps per epoch from UNet in between  $E_{th}^{MUNet}$  and  $Sp_{k}^{MUNet}$ . The term  $DC$  is the dice coefficient and  $JR$  is the jacard index and it is evaluated through Eq. (30) and Eq. (31), respectively.

$$DC = \frac{2 \times A_{po}}{(A_{po} + B_{po}) + (A_{po} + B_{ng})} \quad (30)$$

$$JR = \frac{A_{po}}{A_{po} + B_{po} + B_{ng}} \quad (31)$$

## **B. Ensemble Clustering by Similarity Index**

The abnormal regions of the images are segmented using CNN, Modified UNet and UNet. The resultant segmented images are given to ensemble clustering to obtain the segmented ensemble outcome. The ensemble output is used for calculating the severity level of the disease. More detailed information is obtained from this ensemble output and it is very easy to find the severity level of the brain tumors. The ensemble process accepts the similarity matrix and the similarity matrix is estimated between the mask images and segmented images. The normalized similarity value is determined by applying a log similarity matrix between the images. The structural view of deep learning-based abnormal region segmentation of MRI is given in Fig. 5.

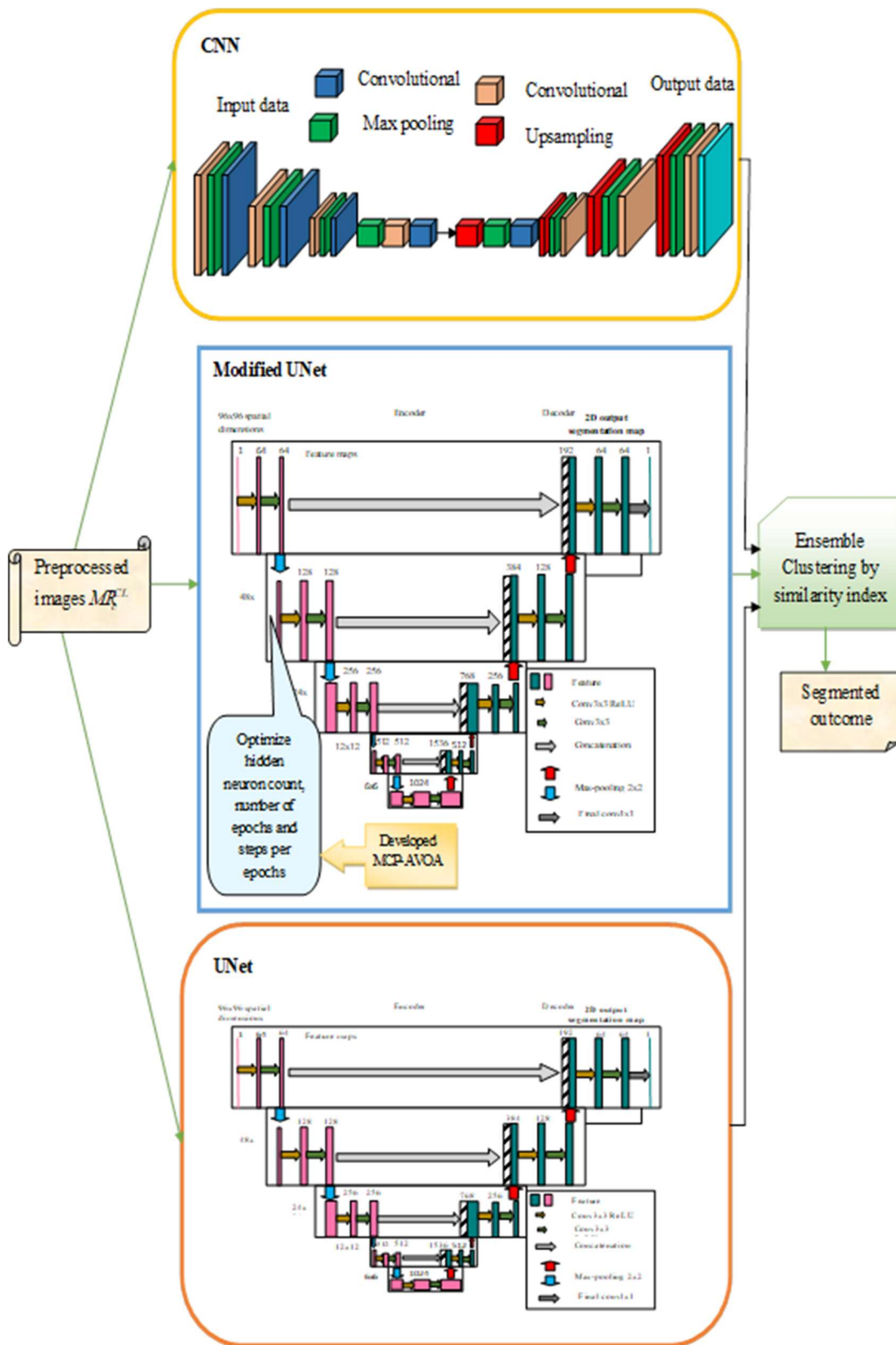


Fig. 5. Block schematic description of deep learning-based abnormal region segmentation

### C. Severity Classification

The severity classification is helpful for discriminating the sets of conditions and it is useful for providing prioritization for patients care. The severity classification is useful for making diagnoses very effectively. In addition, it is helpful for doctors to provide treatment based on the severity level. Based on the severity level of the disease, it is classified into three types like glioma, meningioma and pituitary. The developed MCP-AVOA-TMRAN-based model provides better results in the classification of the severity of brain tumors.

## VI. RESULTS AND DISCUSSIONS

### A. Experimental Setup

The newly designed brain tumor detection and severity classification scheme has been executed in a Python environment. Here, experimental validation has been done to validate the effectiveness of the suggested model. The number of populations to be considered for executing the comparative validation was 10 and the chromosome length has been assumed for executing the experimental analysis was 3. Furthermore, the maximum number of iterations to be assumed for executing the experiments was 50. Traditional algorithms like Mine Blast Optimization (MBO) [27], Archimedes Optimization Algorithm (AOA) [28], Water Strider Algorithm (WSA) [29], and AVOA [26] were considered for the analysis of performance. In addition, the traditional brain tumor detection models with the usage of EfficientNet [1], ResNet [30], DenseNet [31] and TMRAN [32] were also considered for the evaluation of performances.

### B. Efficacy Measures

The performance and computation metrics used for analyzing the effectiveness of the developed model is described as follows.

$$\text{Precision} = \frac{A_{ng}}{A_{po} + B_{po}} \quad (32)$$

$$\text{Sensitivity} = \frac{A_{po}}{A_{po} + B_{po}} \quad (33)$$

$$F - \text{score} = 2 \times \frac{2A_{po}}{2A_{po} + B_{po} + B_{ng}} \quad (34)$$

$$NPV = \frac{A_{ng}}{A_{ng} + B_{ng}} \quad (35)$$

$$MCC = \frac{A_{po} \times A_{ng} - B_{po} \times B_{ng}}{\sqrt{(A_{po} + B_{po})(A_{po} + B_{ng})(A_{ng} + B_{po})(A_{ng} + B_{ng})}} \quad (36)$$

$$\text{Specificity} = \frac{A_{ng}}{A_{ng} + B_{po}} \quad (37)$$

### C. Performance Computation in regards to K-Fold

The performance computation of the developed MCP-AVOA-TMRAN-based brain tumor classification model among various baseline works are illustrated in Fig. 6. The test results revealed that the implemented model provided a higher classification of the accuracy of 6.66%

than EfficientNet, 5.49% than ResNet, 4.34% than DenseNet and 2.12% than TMRAN with the K-Fold value of 2. The f1-score of the developed MCP-AVOA-TMRAN-based brain tumor detection and severity classification model is high and the FPR, as well as FNR, also provides improved results in the developed model than other optimization algorithms.

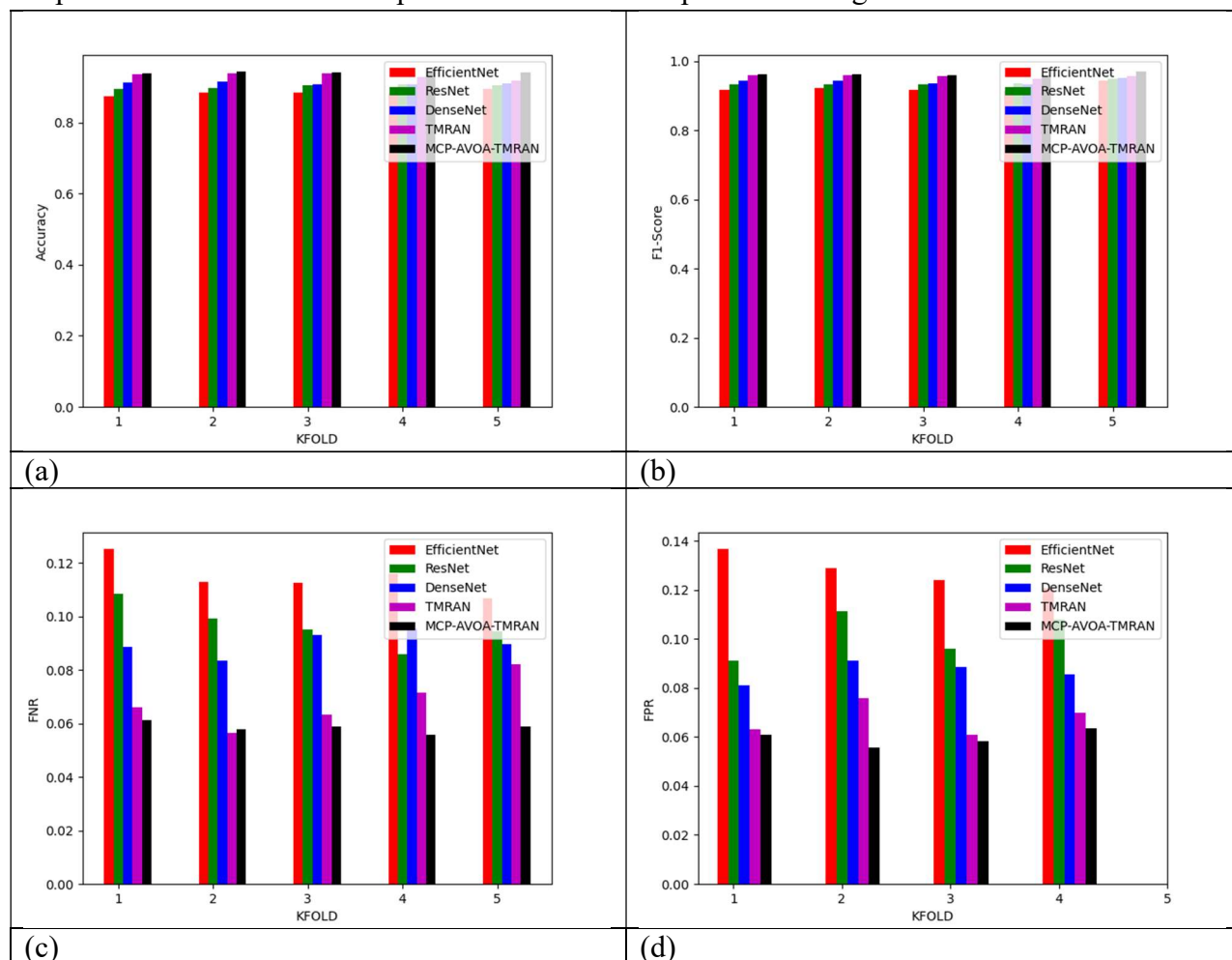


Fig. 6. K-fold validation on recommended Brain Tumor Detection and Severity Classification Model using deep networks among various classifiers in respect to “(a) Accuracy (b) F1-score (c) FNR and (d) FPR.”

#### D. Severity level analysis among various classifiers and optimization algorithms

The severity level of the abnormal region in the proposed MCP-AVOA-TMRAN-based brain tumor classification model in accordance with various classifiers are shown in Fig. 7 and among various optimistic algorithms are depicted in Fig. 8, respectively. The severity level of the diseases is computed based on abnormal levels like glioma, meningioma and pituitary. The analysis graph depicts that the suggested MCP-AVOA-TMRAN-based brain tumor classification model attained with greater accuracy of 5.55% than EfficientNet, 4.39% than ResNet, 3.26% than DenseNet and 1.06% than TMRAN for a meningioma brain tumor. The precision, specificity and sensitivity of

the developed model also highly enhanced with respect to glioma, meningioma and pituitary than other works and algorithms.

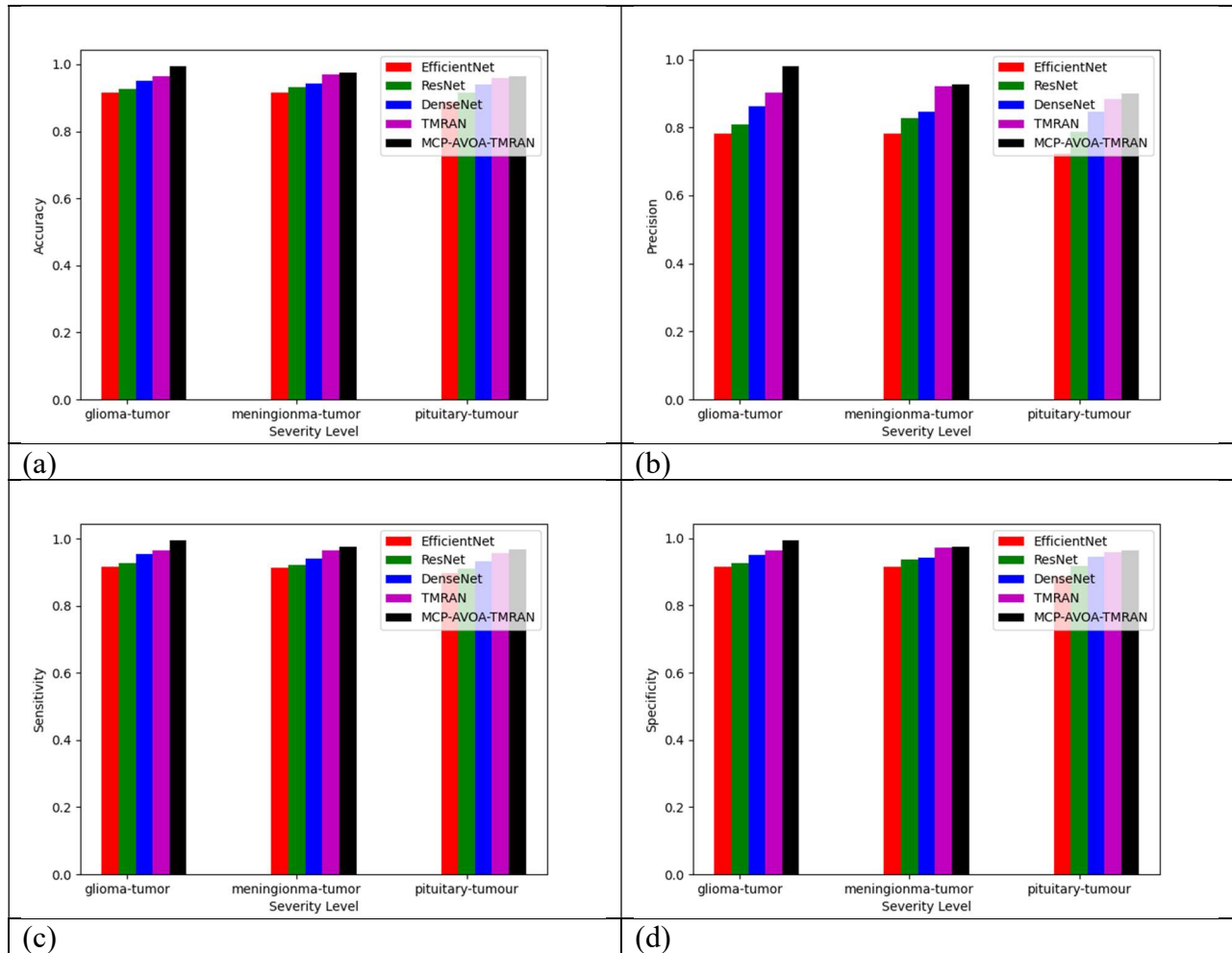


Fig. 7. Severity analysis on recommended Brain Tumor Detection and Severity Classification Model using deep networks among various classifiers in respect to (a) Accuracy (b) Precision (c) Sensitivity and (d) Specificity

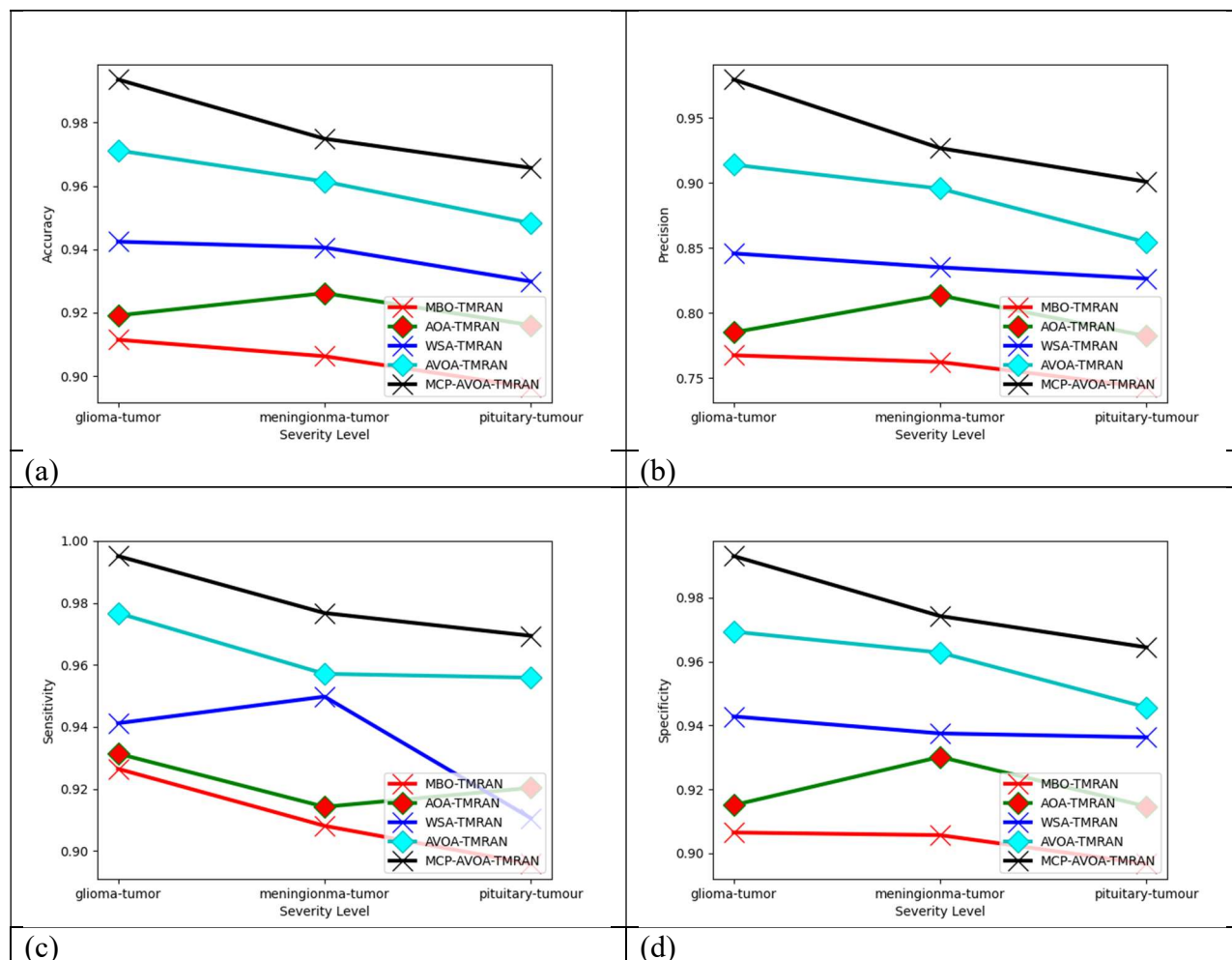


Fig. 8. Severity analysis on recommended Brain Tumor Detection and Severity Classification Model using deep networks among various optimization strategies in respect to (a) Accuracy (b) Precision (c) Sensitivity and (d) Specificity

### E. Cost Function Validation

The cost function validation of the recommended MCP-AVOA-TMRAN-based brain tumor classification framework with respect to various iterations is given in Fig. 9. From the analysis, the performance of the implemented approach is slightly lower in the initial stage of iterations and it performs very well when executing the model in a maximum number of iterations. The empirical results show that it accomplished with improved const function of 16.66% than MBO-TMRAN, 23.07% than AOA-TMRAN, 28.57% than WSA-TMRAN, and 33.33% than AVOA-TMRAN for the iteration value of 20. It converges very faster than the other optimization algorithms used in the analysis.

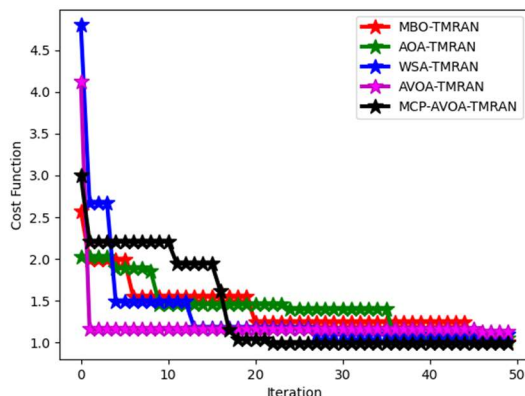


Fig. 9. Cost function validation on recommended Brain Tumor Detection and Severity Classification Model using deep networks among various optimization algorithms

**F. ROC Curve Validation**

The ROC curve validation of the suggested MCP-AVOA-TMRAN-based brain tumor classification framework with respect to abnormal region are given in Fig. 10 (a) and with respect to various severity levels are illustrated in Fig. 10 (b). The baseline brain tumor classification approaches are considered for the analysis of ROC. This analysis is carried out with respect to true positive and false positive rates. The ROC analysis in terms of severity level attained with improved ROC value of 2.56% for EfficientNet, 3.89% than ResNet, 5.26% than DenseNet and 6.66% than TMRAN for the false positive rate value of 0.2 in the abnormal region also, the developed model performed very well when compared to various classifiers.

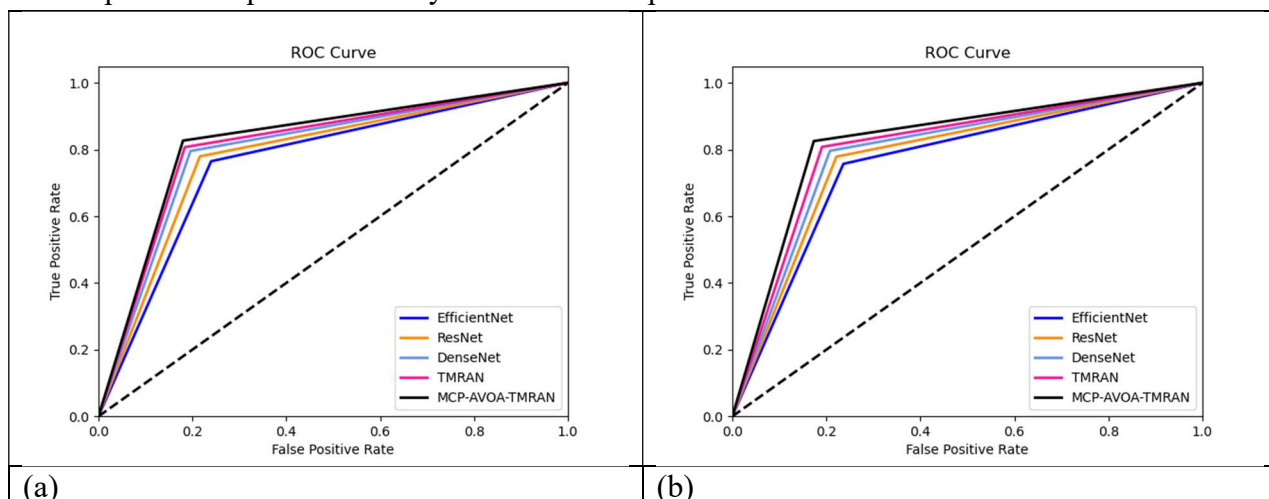


Fig. 10. ROC validation on recommended Brain Tumor Classification Model using deep networks among various optimization algorithms (a) Abnormal classification and (b) Severity classification



**G. Confusion Matrix Validation**

The below Fig.11 depicts the validation of the performance of the suggested MCP-AVOA-TMRAN-based brain tumor classification framework in accordance with the confusion matrix, where the confusion matrix for abnormal is given in Fig. 11 (a) and among severity is plotted in Fig. 11 (b), respectively. The confusion matrix is used for the analysis of accuracy.

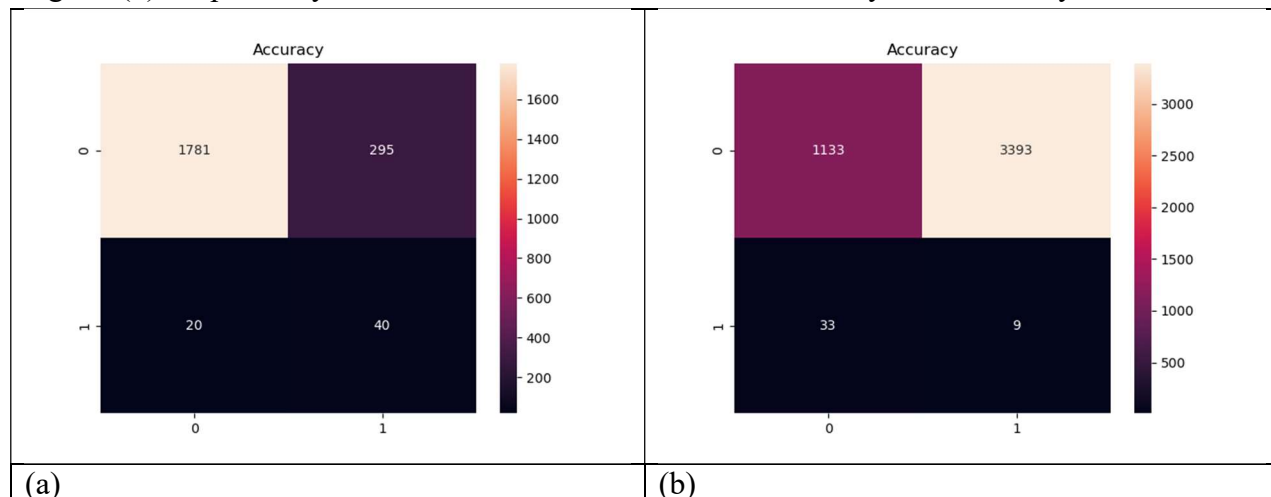
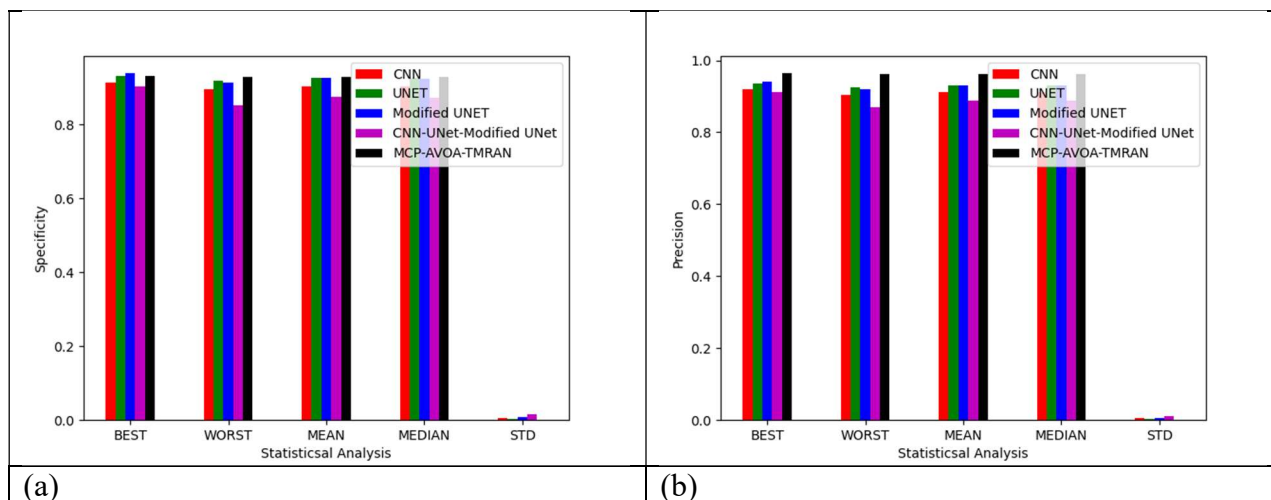


Fig. 11. Confusion Matrix validation on recommended Brain Tumor Detection and Severity Classification Model using deep networks among various optimization algorithms (a) Abnormal classification and (b) Severity classification

**H. Performance Analysis over Segmentation Outcome**

The performance analysis of the segmented MRI images among various classifiers is given in the below Fig. 12. Various measures like specificity, correlation, dice coefficient and specificity are considered for the evaluation of performance. The outcome was shown that the developed model attained with higher segmentation performance than other traditional classifiers.



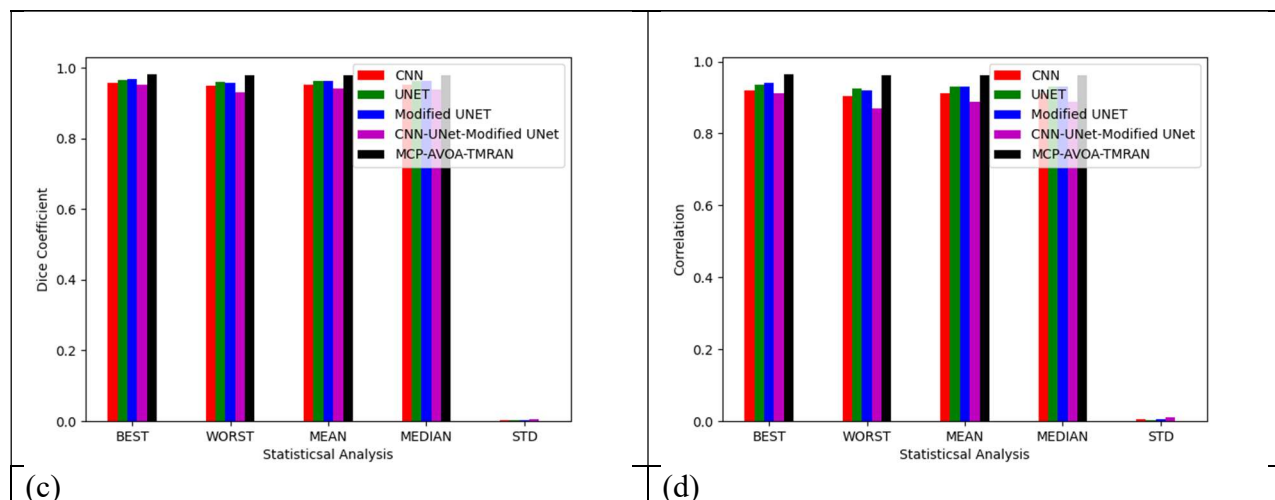


Fig. 12. Performance Analysis segmentation on recommended Brain Tumor Classification Model using deep networks among divergent classifiers in respect to (a) Specificity (b) Precision (c) Dice Coefficient and (d) Correlation

### I. Efficiency Analysis among Various Algorithms and Classifiers

The efficiency of the recommended MCP-AVOA-TMRAN-based brain tumor classification framework in terms of various optimization strategies is given in Table II and various baseline works are depicted in Table III. Here, various positive and negative metrics are considered for the evaluation of performance on developed brain tumor detection schemes. From the tabular analysis, the recommended model attained with extensive accuracy of 9.01% than MBO-TMRAN, 8.10% than AOA-TMRAN, 5.42% than WSA-TMRAN, and 2.30% than AVOA-TMRAN. All the measures have provided more extensive results than the other baseline models during the classification of brain tumors.

**TABLE II. PERFORMANCE COMPUTATION ON DEVELOPED BRAIN TUMOR CLASSIFICATION MODEL AMONG VARIOUS OPTIMIZATION ALGORITHMS**

Performance measures	MBO-TMRAN [27]	AOA-TMRAN [28]	WSA-TMRAN [29]	AVOA-TMRAN [26]	MCP-AVOA-TMRAN
Accuracy	91.14583	91.91176	94.2402	97.1201	99.35662
Sensitivity	92.64706	93.13725	94.11765	97.67157	99.5098
Specificity	90.64542	91.50327	94.28105	96.93627	99.30556
Precision	76.75127	78.5124	84.5815	91.39908	97.94934
FPR	9.354575	8.496732	5.718954	3.063725	0.694444
FNR	7.352941	6.862745	5.882353	2.328431	0.490196
NPV	90.64542	91.50327	94.28105	96.93627	99.30556
FDR	23.24873	21.4876	15.4185	8.600917	2.050663
F1-Score	83.95336	85.20179	89.09513	94.43128	98.7234
MCC	78.57173	80.24269	85.42128	92.58467	98.29886

**TABLE III. PERFORMANCE COMPUTATION ON DEVELOPED BRAIN TUMOR CLASSIFICATION APPROACH AMONG VARIOUS CLASSIFIERS**

Performance measures	EfficientNet [1]	ResNet [30]	DenseNet [31]	TMRAN [32]	ACOA-Hybrid ResGRU	AD-SLno-VGG-Ensemble	FMATSO - MDDTCN
Accuracy	91.54412	92.6777	95.09804	96.53799	97.2332	98.81423	99.35662
Sensitivity	91.66667	92.76961	95.46569	96.56863	97.41935	98.70968	99.5098
Specificity	91.50327	92.64706	94.97549	96.52778	96.93878	98.97959	99.30556
Precision	78.24268	80.78975	86.36364	90.26346	98.05195	99.35065	97.94934
FPR	8.496732	7.352941	5.02451	3.472222	3.061224	1.020408	0.694444
FNR	8.333333	7.230392	4.534314	3.431373	2.580645	1.290323	0.490196
NPV	91.50327	92.64706	94.97549	96.52778	96.93878	98.97959	99.30556
FDR	21.75732	19.21025	13.63636	9.736541	1.948052	0.649351	2.050663
F1-Score	84.42438	86.36623	90.68685	93.30965	97.73463	99.02913	98.7234
MCC	79.13531	81.75709	87.57372	91.0724	94.18468	97.50969	98.29886

**J. Statistical Estimation on Heuristic Algorithms**

The efficacy of the recommended brain tumor detection system among various optimization strategies are demonstrated in Table IV. Various statistical metrics are evaluated for the validation of performance on the recommended MCP-AVOA-TMRAN-based brain tumor classification framework and the analysis shows that the recommended model obtained with enhanced median value of 20.76% than MBO-TMRAN, 29.53% than AOA-TMRAN, 16.12% than WSA-TMRAN, and 14.66% than AVOA-TMRAN. The efficiency of the recommended brain tumor detection scheme has enhanced than the other heuristic algorithms.

**TABLE IV. STATISTICAL COMPUTATION ON DEVELOPED BRAIN TUMOR CLASSIFICATION MODEL AMONG VARIOUS ALGORITHMS**

Performance measures	MBO-TMRAN [27]	AOA-TMRAN [28]	WSA-TMRAN [29]	AVOA-TMRAN [26]	MCP-AVOA-TMRAN
Best	1.000857	1.045588	1.094176	1.12289	0.987383

Worst	2.572905	2.027521	4.798819	4.125907	1.001301
Mean	1.407077	1.417572	1.357385	1.213675	1.387724
Median	1.24622	1.401141	1.177177	1.157028	0.987383
Std	0.309844	0.301292	0.620337	0.416136	0.565183

## VII. CONCLUSION

A new brain tumor classification model has been designed for identifying normal and multi-class brain tumors from MRI images with higher classification accuracy. Three different benchmark datasets were used for classifying the severity of brain tumors from the MRI images. The collected images were preprocessed through median filtering and CLAHE for enhancing the quality of the images. Then, the TMRAN network has been adopted for classifying the MRI images to provide results about normal and abnormal. Here, the parameters from TMRAN were optimized via MCP-AVOA to maximize classification accuracy. The classified images have been applied to the segmentation stage, where the CNN, Modified UNet and UNet have been utilized for the segmentation of images. The parameters from Modified UNet have been tuned via MCP-AVOA for enhancing the dice coefficient as well as the Jacard index. Performance comparison has been done to validate the efficiency of the developed model and the results were revealed that the suggested approach accomplished with enhanced accuracy of 8.53% than EfficientNet, 7.20% than ResNet, 4.47% than DenseNet and 2.91% than TMRAN, 2.18% than ACOA-Hybrid ResGRU and 0.54% than AD-SLno-VGG-Ensemble. The performance of the implemented approach is highly enhanced among various classifiers and algorithms while processing the classification of brain tumors.

## References

- [1] H. A. Shah, F. Saeed, S. Yun, J. -H. Park, A. Paul and J. -M. Kang, "A Robust Approach for Brain Tumor Detection in Magnetic Resonance Images Using Finetuned EfficientNet," IEEE Access, vol. 10, pp. 65426-65438, 2022.
- [2] A. S. Musallam, A. S. Sherif and M. K. Hussein, "A New Convolutional Neural Network Architecture for Automatic Detection of Brain Tumors in Magnetic Resonance Imaging Images," in IEEE Access, vol. 10, pp. 2775-2782, 2022.
- [3] M. V. S. Ramprasad, M. Z. U. Rahman and M. D. Bayleyegn, "A Deep Probabilistic Sensing and Learning Model for Brain Tumor Classification With Fusion-Net and HFCMIK Segmentation," IEEE Open Journal of Engineering in Medicine and Biology, vol. 3, pp. 178-188, 2022.
- [4] P. Kumar Mallick, S. H. Ryu, S. K. Satapathy, S. Mishra, G. N. Nguyen and P. Tiwari, "Brain MRI Image Classification for Cancer Detection Using Deep Wavelet Autoencoder-Based Deep Neural Network," in IEEE Access, vol. 7, pp. 46278-46287, 2019.
- [5] Atish Chaudhary & Vandana Bhattacharjee, "An efficient method for brain tumor detection and categorization using MRI images by K-means clustering & DWT," International Journal of Information Technology, vol. 12, pp.141–148, 2020.

- [6] K. C. Manoj & D. Anto Sahaya Dhas, "Automated brain tumor malignancy detection via 3D MRI using adaptive-3-D U-Net and heuristic-based deep neural network," *Multimedia Systems*, vol.28, pp.2247–2273, 2022.
- [7] S. Deepak & P. M. Ameer, "Automated Categorization of Brain Tumor from MRI Using CNN features and SVM," *Journal of Ambient Intelligence and Humanized Computing*, vol. 12, pp.8357–8369, 2021.
- [8] Javaria Amin, Muhammad Sharif, Mudassar Raza, Tanzila Saba, Rafiq Sial & Shafqat Ali Shad, "Brain tumor detection: a long short-term memory (LSTM)-based learning model," *Neural Computing and Applications*, vol.32, pp.15965–15973, 2020.
- [9] A. Gokulalakshmi, S. Karthik, N. Karthikeyan & M. S. Kavitha, "ICM-BTD: improved classification model for brain tumor diagnosis using discrete wavelet transform-based feature extraction and SVM classifier," *Soft Computing*, vol. 24, pp.18599–18609, 2020.
- [10] Abdulkadir Karacı & Kemal Akyol, "YoDenBi-NET: YOLO + DenseNet + Bi-LSTM-based hybrid deep learning model for brain tumor classification," *Neural Computing and Applications*, vol. 35, pp.12583–12598, 2023.
- [11] Emrah Irmak, "Multi-Classification of Brain Tumor MRI Images Using Deep Convolutional Neural Network with Fully Optimized Framework," *Iranian Journal of Science and Technology, Transactions of Electrical Engineering* vol. 45, pp.1015–1036, 2021.
- [12] Sohaib Asif, Ming Zhao, Fengxiao Tang & Yusen Zhu, "An enhanced deep learning method for multi-class brain tumor classification using deep transfer learning," *Multimedia Tools and Applications*, 2023.
- [13] Rajeev Kumar Gupta, Santosh Bharti, Nilesh Kunhare, Yatendra Sahu & Nikhlesh Pathik, "Brain Tumor Detection and Classification Using Cycle Generative Adversarial Networks," *Interdisciplinary Sciences: Computational Life Sciences*, vol. 14, pp.485–502, 2022.
- [14] Sumeet Saurav, Ayush Sharma, Ravi Saini & Sanjay Singh, "An attention-guided convolutional neural network for automated classification of brain tumor from MRI," *Neural Computing and Applications*, vol. 35, pp.2541–2560, 2023.
- [15] G. J. Ferdous, K. A. Sathi, M. A. Hossain, M. M. Hoque and M. A. A. Dewan, "LCDEiT: A Linear Complexity Data-Efficient Image Transformer for MRI Brain Tumor Classification," *IEEE Access*, vol. 11, pp. 20337-20350, 2023.
- [16] J. J. Corso, E. Sharon, S. Dube, S. El-Saden, U. Sinha and A. Yuille, "Efficient Multilevel Brain Tumor Segmentation With Integrated Bayesian Model Classification," *IEEE Transactions on Medical Imaging*, vol. 27, no. 5, pp. 629-640, May 2008.
- [17] A. Gumaei, M. M. Hassan, M. R. Hassan, A. Alelaiwi and G. Fortino, "A Hybrid Feature Extraction Method With Regularized Extreme Learning Machine for Brain Tumor Classification," *IEEE Access*, vol. 7, pp. 36266-36273, 2019.
- [18] N. Noreen, S. Palaniappan, A. Qayyum, I. Ahmad, M. Imran and M. Shoaib, "A Deep Learning Model Based on Concatenation Approach for the Diagnosis of Brain Tumor," *IEEE Access*, vol. 8, pp. 55135-55144, 2020.

- [19] A. Islam, S. M. S. Reza and K. M. Iftekharuddin, "Multifractal Texture Estimation for Detection and Segmentation of Brain Tumors," *IEEE Transactions on Biomedical Engineering*, vol. 60, no. 11, pp. 3204-3215, Nov. 2013.
- [20] S. Asif, W. Yi, Q. U. Ain, J. Hou, T. Yi and J. Si, "Improving Effectiveness of Different Deep Transfer Learning-Based Models for Detecting Brain Tumors From MR Images," in *IEEE Access*, vol. 10, pp. 34716-34730, 2022.
- [21] C. Ge, I. Y. -H. Gu, A. S. Jakola and J. Yang, "Enlarged Training Dataset by Pairwise GANs for Molecular-Based Brain Tumor Classification," in *IEEE Access*, vol. 8, pp. 22560-22570, 2020.
- [22] N. Micallef, D. Seychell and C. J. Bajada, "Exploring the U-Net++ Model for Automatic Brain Tumor Segmentation," in *IEEE Access*, vol. 9, pp. 125523-125539, 2021.
- [23] B. Devanathan & M. Kamarasan, "Multi-objective Archimedes Optimization Algorithm with Fusion-based Deep Learning model for brain tumor diagnosis and classification," *Multimedia Tools and Applications*, vol. 82, pp.16985–17007, 2023.
- [24] Muhammad Irfan Sharif, Jian Ping Li, Muhammad Attique Khan, Seifedine Kadry & Usman Tariq, "M3BTCNet: multi model brain tumor classification using metaheuristic deep neural network features optimization," *Neural Computing and Applications*, 2022.
- [25] Mantripragada Yaswanth Bhanu Murthy, Anne Koteswararao & Melingi Sunil Babu, "Adaptive fuzzy deformable fusion and optimized CNN with ensemble classification for automated brain tumor diagnosis," *Biomedical Engineering Letters*, vol.12, pp.7–58, 2022.
- [26] Benyamin Abdollahzadeh, Farhad Soleimanian Gharehchopogh, Seyedali Mirjalili, "African vultures optimization algorithm: A new nature-inspired metaheuristic algorithm for global optimization problems," *Computers & Industrial Engineering*, Vol. 158, August 2021.
- [27] M. Shahrouzi, A. Meshkat-Dini and A. Azizi, "Optimal Wind Resistant Design of Tall Buildings Utilizing Mine Blast Algorithm," *International Journal of Optimization In Civil Engineering*, vol.5, Issue.2, pp.137-150, 2014.
- [28] Fatma A. Hashim, Kashif Hussain, Essam H. Houssein, Mai S. Mabrouk & Walid Al-Atabany, "Archimedes optimization algorithm: a new metaheuristic algorithm for solving optimization problems," *Applied Intelligence*, vol. 51, pp.1531–1551, 2021.
- [29] A. Kaveh, and A. Dadras Eslamlou, "Water strider algorithm: A new metaheuristic and applications," *Structures*, vol.25, pp. 520-541, June 2020.
- [30] T. Kalaiselvi, S.T. Padmapriya, "Multimodal MRI Brain Tumor Segmentation—A ResNet-based U-Net approach," *Brain Tumor MRI Image Segmentation Using Deep Learning Techniques*, pp. 123-135, 2022.
- [31] Yufan Zhou, Zheshuo Li, Hong Zhu, Changyou Chen, Mingchen Gao, Kai Xu, and Jinhui Xu, "Holistic Brain Tumor Screening and Classification Based on DenseNet and Recurrent Neural Network," *LNCS 11383*, pp. 208–217, 2019.
- [32] Zhaopan Li, Junfeng Li, And Wenzhan Dai, "A Two-Stage Multiscale Residual Attention Network for Light Guide Plate Defect Detection," *IEEE Access*, vol. 9, 2021.

- [33] Baris, Kayalibay, Grady Jensen, Patrick van der Smag, "CNN-based Segmentation of Medical Imaging Data," 2017.
- [34] Batyrkhan Omarov Azhar Tursynova, Octavian Postolache, Khaled Gamry, Aidar Batyrbekov, Sapargali Aldeshov, Zhanar Azhibekova, Marat Nurtas, Akbayan Aliyeva and Kadrzhan Shiyapov, "Modified UNet Model for Brain Stroke Lesion Segmentation on Computed Tomography Images," CMC, vol.71, no.3, 2022.
- [35] Libin Jiao, Lianzhi Huo, Changmiao Hu and Ping Tang, "Refined UNet: UNet-Based Refinement Network for Cloud and Shadow Precise Segmentation," Remote Sensing, 2020.